AUTOMATED CARDIAC SUPPORT SYSTEM: REAL-TIME ECG MONITORING AND AUTOMATED CPR USING FPGA AND LIDAR TECHNOLOGIES

Pranabesh Bhattacharjee[1], Tanmay Sindhwani[1], and Aniruddha Datta[1]
[1]Department of Electrical and Computer Engineering, TAMU, College Station, Texas 77843-3128, USA

Corresponding Author: Pranabesh Bhattacharjee
Email: p.bhattacharje@tamu.edu

ABSTRACT

Complications during surgery or severe medical conditions often require immediate intervention to prevent adverse outcomes. This study proposes a simulation-based framework for an automated cardiac support system that integrates real-time heart rate monitoring, CPR actuation, and drug delivery using advanced technologies. The system utilizes an FPGA-based controller to process patient data from ECG sensors and pulse oximeters, enabling multi-parameter decision-making based on heart rate and oxygen saturation levels. Bradycardia (<50 bpm with SpO_2 <95%) triggers automated CPR, while tachycardia (>120 bpm with SpO_2 ≥95%) activates intravenous drug delivery of adenosine, followed by a saline flush. LiDAR technology is employed to precisely map the patient's chest contours, ensuring optimal placement and alignment of the CPR device for effective compressions. MATLAB simulations validate the accuracy of LiDAR-based chest mapping with an error margin of ±2 mm, while FPGA simulations demonstrate timely responsiveness with CPR activation occurring within 10 ns and drug delivery also initiated within 10 ns. The results highlight the feasibility of integrating these technologies into a unified framework for real-time cardiac support. While this study is limited to simulations conducted using LabVIEW, MATLAB, and Xilinx Vivado, it provides a theoretical foundation for future prototyping and experimental validation using CPR manikins and intravenous drug setups. This approach has the potential to revolutionize emergency response protocols by offering reliable and cost-effective automated cardiac care in critical settings.

Keywords: Cardiac assist system, CPR, ECG, FPGA, LiDAR, LUCAS.

1. INTRODUCTION

Cardiac complications during surgery pose significant risks to patient safety, often requiring immediate and effective intervention to prevent adverse outcomes. Traditional methods heavily depend on the swift response of medical personnel to administer CPR and appropriate drugs, which can be particularly challenging in the time-sensitive environment of an operating room [1]. Recent advancements in medical technology offer opportunities to automate and enhance these critical responses, potentially improving patient outcomes even outside a hospital [2]. This paper explores the development of an automated emergency CPR support system equipped with an integrated drug delivery mechanism. The system continuously monitors the heart rate of a patient undergoing an operation or in a severe medical condition, using predefined thresholds to trigger CPR when the heart rate drops critically low and administer drugs when the heart rate exceeds safe limits. This dual-function approach aims to provide seamless cardiac support, reduce the workload on medical staff, and increase the chances of patient survival during cardiac events.

Automated CPR devices are designed to ensure consistent and effective chest compressions during cardiac arrest, making a critical difference in life-threatening situations. One such device, the LUCAS (Lund University Cardiac Assist System), has become a trusted tool in emergency medical services and hospitals. Unlike manual CPR, which can vary in quality due to fatigue or human error, devices like LUCAS consistently deliver reliable compressions, improving the chances of patient survival [3], which

can be crucial in maintaining perfusion during cardiac arrest. However, these devices are primarily used in pre-hospital and emergency settings and are not typically integrated with surgical procedures or automated drug delivery systems. Automated drug delivery systems have been gaining attention for their ability to adjust medication administration based on real-time physiological data. In the context of cardiac care, such systems have been explored for delivering antiarrhythmic drugs and managing blood pressure [4]. For instance, insulin pumps in diabetes management have successfully demonstrated the efficacy of automated drug delivery [5]. While these systems showcase the potential of automation (under medical team administration) in medical applications, their integration with emergency CPR systems remains limited. Intraoperative cardiac monitoring is essential for detecting and responding to hemodynamic changes during surgery. Technologies such as electrocardiography (ECG) and pulse oximetry are standard in operating rooms to monitor heart rate and oxygen saturation. Monitoring SpO_2 provides critical insights into peripheral perfusion and oxygen delivery to tissues, enabling timely detection of hypoxemia, which may exacerbate cardiac complications during surgery or emergencies. Advanced monitoring systems leverage machine learning algorithms to forecast cardiac events, facilitating proactive medical interventions. For example, a study in npj Digital Medicine introduced and validated a real-time machine learning model for predicting in-hospital cardiac arrests using ECG-based heart rate data [7]. This model showed remarkable potential for early detection, enabling prompt medical action. Additionally, a meta-analysis published in Scientific reports emphasizes the effective predictive capabilities of machine learning algorithms, particularly support vector machines and boosting methods, in cardiovascular diseases [8]. These insights highlight the significant role of machine learning in improving the accuracy of cardiac event predictions.

Despite these advancements, there is a need for systems that not only monitor but also autonomously respond to critical cardiac events by initiating CPR and administering drugs. This study introduces a conceptual model for integrating automated CPR with drug delivery systems, aiming to evaluate its theoretical feasibility and potential impact. Existing research has primarily focused on individual components, such as mechanical/auto CPR devices [9] or app-based drug delivery systems [10], rather than a combined approach. A few studies have explored the potential benefits of such integration in improving patient outcomes during cardiac arrest [11][12]. As the integration of automated CPR with drug delivery is a relatively novel concept, our work establishes a theoretical framework, providing a foundation for future prototyping and experimental validation.

This paper takes only the initial step in that direction. FPGA (Field-Programmable Gate Array)-based systems have gained significant attention in health monitoring applications due to their flexibility, real-time processing capabilities, and low latency. These systems are particularly well-suited for applications requiring real-time bio-signal processing, such as ECG (electrocardiogram) and SpO_2 monitoring, where FPGAs efficiently handle signal acquisition, filtering, and QRS complex detection, enabling arrhythmia classification and heart rate variability analysis [13]. Similarly, EEG (electroencephalogram) monitoring systems leverage FPGAs for real-time brainwave analysis, supporting applications like seizure detection and brain-computer interfaces [14]. In wearable health monitoring devices, FPGAs process data from multiple sensors to track vital signs, including heart rate, blood pressure, and blood oxygen saturation (SpO_2), while enabling wireless communication for remote health tracking [15]. Moreover, FPGAs are utilized in advanced medical imaging modalities, such as ultrasound and CT systems, to accelerate image processing and enhance diagnostic capabilities [16]. Their inherent advantages, including parallel processing, reconfigurability, and low power consumption, make FPGAs an ideal choice for multi-parameter health monitoring systems that combine ECG, EEG, and temperature data into a single platform [17]. These characteristics highlight the potential of FPGA-based solutions in improving real-time health

monitoring and diagnosis. This work focuses on developing a simulation-based framework for an automated cardiac support system. The proposed system modeled using LabVIEW, MATLAB, and Xilinx Vivado, demonstrates the feasibility of integrating real-time heart rate and blood oxygen level monitoring, CPR actuation, and automated drug delivery. While this study does not include physical hardware implementation, it provides a theoretical foundation for future prototyping and experimental validation upon securing funding. Unlike existing systems that focus on individual components such as mechanical CPR devices or automated drug delivery units, this work integrates these functionalities into a unified framework controlled by an FPGA. The novelty lies in combining real-time heart rate monitoring with LiDAR-based chest mapping (simulated in MATLAB) and dynamic drug dosage computation (modeled in Verilog). The subsequent section provides an in-depth discussion of the integration of automated CPR with drug delivery based on an FPGA-based controller.

2. METHODOLOGY

The proposed emergency CPR support system with integrated drug delivery is designed to provide real-time cardiac support for patients during and after surgery. A flowchart indicating the steps involved shown in Fig. 1. The system consists of four main components: a heart rate monitoring module (ECG machine), a CPR actuation mechanism, an automated drug delivery unit, and a FPGA based controller to control and keep track of heartbeats and initiate the CPR system or drug delivery based on real-time anomalies. The detailed procedure is described in the following sub-sections.

2.1 Heart Rate Monitoring Module

The system uses high-precision electrocardiography (ECG) sensors to continuously monitor the patient's heart rate and rhythm. Additional sensors, such as pulse oximeters, provide supplementary data on oxygen saturation levels (SpO_2). The FPGA-based controller [18] processes data from both sensors in real time using algorithms programmed to detect abnormal conditions such as bradycardia (<50 bpm with SpO_2 <95%) or tachycardia (>120 bpm with $SpO_2 \geq 95\%$) [19]. By combining these parameters, the system ensures that decisions are made based on comprehensive physiological data rather than relying solely on heart rate thresholds.

2.2 CPR Actuation Mechanism

The LUCAS chest compression system [20] is integrated into the system to deliver chest compressions. The device is positioned over the patient's chest and operates based on predefined compression depth and rate settings. We used LiDAR (Light Detection and Ranging) [21] based detection for auto-measuring the area of the chest to fit it properly to get the maximum therapeutic benefit. We programmed the LiDAR based CPR actuation in MATLAB platform, all the measurement calculation is discussed in more detail later in the results section. When the heart rate monitoring module (FPGA controller) detects bradycardia, the system activates the mechanical CPR device to initiate chest compressions. The device continues to operate until the heart rate returns to a safe level or medical personnel intervene. The LiDAR-based chest mapping process uses mathematical modeling to ensure precise alignment with patient contours, as described in detail in section 3.1.

2.3 Automated Drug Delivery Unit

The system includes reservoirs for storing emergency medications. We used "Adenosine" [22] as a drug because it does not make the blood thin [23]; if this were allowed to happen then the patient could die during the surgery due to excessive bleeding. Precision pumps are used to administer these drugs intravenously. We programmed the FPGA with a Verilog code to control the bradycardia and tachycardia situation effectively. Both the MATLAB and Verilog codes are available in the following GitHub repository: https://github.com/PranabeshTAMU/Automated_CPR. The Verilog code of the FPGA

controller determines the drug dosage based on heart rate data. The whole system model is shown on Fig.2. We discussed the main algorithm of our code in the subsection below.

2.4 Detection and Decision-Making by the FPGA Controller

The algorithm continuously compares the heart rate to a predefined low threshold. If the heart rate drops below this threshold, the system classifies it as bradycardia and triggers the CPR actuation mechanism (Fig. 3). Similarly, the algorithm monitors heart rates exceeding a predefined high threshold. If the heart rate is too high, it triggers the drug delivery unit to administer a calming medication. CPR initiation starts upon detecting bradycardia, the algorithm sends a command to the CPR device to start compressions (Fig. 3). The device operates according to ACLS (Advanced Cardiac Life Support) guidelines [24]. Drug administration is initiated by tachycardia, the algorithm determines the appropriate drug and dosage. The system is designed to factor in patient-specific parameters such as weight, age, and medical history to personalize treatment. These parameters can be defined by the medical administration team to tailor drug dosage and interventions more accurately. However, in this simulation-based study, we did not use these patient-specific parameters. Instead, we relied on predefined drug doses as outlined in Table 3 (e.g., 6 mg for initial adenosine administration and 12 mg for a second dose if required). These predefined doses align with standard medical protocols for treating supraventricular tachycardia (SVT). Future work will involve incorporating patient-specific parameters into the system to enable dynamic and personalized decision-making during real-world applications.

2.5 System block diagram

This diagram (Fig.2) provides a high-level view of the entire system, showing the main components and their interconnections. The first one is the heart rate monitoring module consisting of ECG sensors, a data processor (inside the ECG machine itself, which provides all the collected data in real time), a CPR actuation mechanism which consists of a mechanical CPR device and a LiDAR, a control unit, a drug delivery unit with drug reservoirs and precision pumps. Both the modules are connected with a FPGA based central control unit. The heart rate monitoring module focuses on the components and connections within the heart rate monitoring module, which includes ECG sensors connected to the patient through lead wires, a signal conditioning circuit, and a data processor (controller) equipped with an analog-to-digital converter (ADC) and a heart rate detection algorithm [25]. The connections are as follows: ECG sensors connect to the signal conditioning circuit, which then connects to the ADC. The ADC is linked to the controller, which communicates with the central control unit (Table 1). For the experiment that we carried out, we considered a mechanical CPR, which includes a motor/actuator, a compression pad, and a control unit featuring a motor driver and LiDAR feedback sensors (for positioning), and we activated it through the FPGA controller (Central control unit) when the bradycardia occurred. The central control unit (FPGA) connects to the LiDAR based control unit of the auto CPR, which links to the motor driver. The motor driver then connects to the motor/actuator, which is attached to the compression pad. Feedback sensors connect back to the control unit [26]. The automated drug delivery unit block diagram (Fig. 2) illustrates the components and connections within the drug delivery unit, which consists of multiple drug reservoirs and precision pumps (such as peristaltic or syringe pumps) components and processes, and it is similar like a continuous glucose monitor insulin pumps [27]. The following is a detailed description of how such a device consisting of the following components would work: LiDAR sensors, data processor (MATLAB-based), mechanical CPR device, control algorithm, and central control unit (FPGA controller). The CPR device is placed on or near the patient's chest. The LiDAR sensors are activated to start scanning the chest. LiDAR sensors emit laser pulses and measure the time it takes for the pulses to return [28], mapping the chest area. The data processor creates a detailed 3D model of the chest. The LiDAR analyzes the chest dimensions and contour based on the 3D model, the adjustable pads on the mechanical CPR

device expand or contract to fit the chest snugly. ensures that the device is correctly positioned for optimal compression, and this guarantees that the CPR device fits perfectly over the chest, maximizing effectiveness. Realtime adjustments are made to maintain correct placement and force, adjust in real-time to any changes in the chest contour during CPR, and maintain optimal performance. By integrating LiDAR technology with advanced control systems, this automated CPR device could significantly improve the precision and effectiveness of life-saving chest compressions in emergencies. The central control unit processes the heart rate data using decision-making algorithms to determine if CPR or drug delivery is needed. If CPR is required, the central control unit sends a control signal to the CPR actuation mechanism to initiate chest compressions. If drug delivery is needed, the central control unit sends a control signal to the automated drug delivery Unit to administer the appropriate medication.

The following section presents simulated results from MATLAB and FPGA implementations, validating the feasibility of our proposed system.

3. RESULTS

In the previous section, it is shown how the proposed model works for a patient who is undergoing an operation/surgery and what the interconnection blocks of the proposed system are. In this section, the simulated result of the controller and the LiDAR-based chest area mapping is shown for auto CPR.

3.1 CPR auto adjustment with LiDAR scanner

LiDAR technology enables precise mapping of the patient's chest by generating a dense point cloud representing its 3D geometry. To ensure accurate alignment of the CPR device, mathematical modeling is used to fit an ellipsoid to this data. In the context of LiDAR detection, an ellipsoid can be used to model the shape and distribution of points in a point cloud [29]. A LiDAR point cloud is a collection of data points in 3D space, typically generated by a LiDAR scanner that emits laser beams and measures the reflected signals to calculate distances. Each point in the cloud represents a position in 3D space and is characterized by its (x, y, z) coordinates. The LiDAR scanner collects a dense set of 'N' points, typically corresponding to the surface of an object—in this case, the patient's chest or any other target area for CPR adjustment. An ellipsoid is a three-dimensional geometric shape that resembles a stretched or compressed sphere, and it can be mathematically defined by its center, three principal radii (semi-axes), and orientation. It is used to fit the CPR object over the patient's chest. An ellipsoid centered at (x_0, y_0, z_0) with semi-axes a, b, and c aligned along the coordinate axes can be described by the equation:

$$\frac{(x-x_0)^2}{a^2}+\frac{(y-y_0)^2}{b^2}+\frac{(z-z_0)^2}{c^2}=1 \qquad \text{(eq. 1)}$$

Fitting an ellipsoid to a LiDAR point cloud typically involves the following steps: Collect the LiDAR point cloud data, which consists of points (x_i, y_i, z_i). The centroid of the point cloud is calculated by taking the average of the x, y, z coordinates of all N points:

$$x_0=\frac{1}{N}\sum_{i=1}^{N}x_i,\ y_0=\frac{1}{N}\sum_{i=1}^{N}y_i,\ z_0=\frac{1}{N}\sum_{i=1}^{N}z_i, \qquad \text{(eq. 2)}$$

where N is the number of points, defines the size of the dataset being used to fit the ellipsoid. A larger N generally leads to better accuracy in modeling the surface shape because more data points allow the ellipsoid fitting algorithm to capture fine details of the 3D geometry. The higher the N, the more precise the ellipsoid fitting will be, ensuring the CPR device aligns accurately with the chest curvature.

Calculation of the covariance matrix of the centered data points:

$$C=\frac{1}{N}\sum_{i=1}^{N}\begin{pmatrix}(x_i-x_0)^2 & (x_i-x_0)(y_i-y_0) & (x_i-x_0)(z_i-z_0)\\ (y_i-y_0)(x_i-x_0) & (y_i-y_0)^2 & (y_i-y_0)(z_i-z_0)\\ (z_i-z_0)(x_i-x_0) & (z_i-z_0)(y_i-y_0) & (z_i-z_0)^2\end{pmatrix} \qquad \text{(eq. 3)}$$

where C is the covariance matrix. Now perform eigen decomposition on the covariance matrix C:

$$C = Q\Lambda Q^T \qquad \text{(eq. 4)}$$

where Q is the matrix of eigenvectors and Λ is the diagonal matrix of eigenvalues. The lengths of the semi-axes a, b, and c are related to the eigenvalues λ1, λ2, and λ3 of the covariance matrix:

$$a = \sqrt{\lambda_1}, b = \sqrt{\lambda_2}, c = \sqrt{\lambda_3} \qquad \text{(eq. 5)}$$

The orientation of the ellipsoid is given by the eigenvectors in Q. Combining the center, semi-axes, and orientation, the equation of the ellipsoid in its general form (considering rotation) can be written as:

$$X^T AX = 1 \qquad \text{(eq. 6)}$$

where, $X = (x - x_0)$ and $A = Q\Lambda^{-1}Q^T$ which is derived from the eigenvalues and eigenvectors of the covariance matrix. The covariance matrix of the centered LiDAR point cloud data is calculated using Equation (3), where CC represents the variability of the points in each dimension. This matrix is essential for determining the shape and orientation of the ellipsoid that fits the data. Eigen decomposition of C, as shown in Equation (4), yields eigenvalues (λ_1, λ_2, λ_3) and eigenvectors (Q), which correspond to the semi-axis lengths (a, b, c) and orientation of the ellipsoid. These parameters are used to accurately model the patient's chest contour for optimal CPR device positioning. An example of this LiDAR point cloud and fitted ellipsoid parameters is shown on Table 2 and the 3D ellipsoid model generated by using the MATLAB code is shown in Fig. 4, the MATLAB code is available at the following GitHub repository: https://github.com/PranabeshTAMU/Automated_CPR. LiDAR technology enables precise mapping of the patient's chest by generating a dense point cloud representing its 3D geometry. MATLAB simulations validate that this approach achieves an average error margin of ±2 mm in chest contour alignment, ensuring optimal placement of the CPR device.

3.2 FPGA simulation results based on ECG sensor's real-time data of the patient

We assume that the system is fully connected to the patient's body, enabling real-time monitoring and intervention. The heart rate and oxygen saturation (SpO_2) levels are continuously monitored using ECG sensors and pulse oximeters, ensuring comprehensive physiological data for decision-making. Using LiDAR-based detection, the CPR device adjusts its position over the patient's chest to ensure accurate compressions. Meanwhile, an intravenous drug delivery module is positioned on the patient's arm for rapid medication administration.

Figure 3 illustrates how the FPGA system monitors heart rate and oxygen saturation levels using ECG sensors and pulse oximeters. Bradycardia (<50 bpm with SpO_2 <95%) triggers CPR activation, while tachycardia (>120 bpm with SpO_2 ≥95%) initiates drug delivery. When the heartbeat is within the normal range (50–120 beats per minute), and SpO_2 levels are ≥95%, the controller remains inactive (Fig. 3), meaning neither the drug delivery nor CPR system is activated.

An intravenous line (IV) inserted into a vein, typically in the patient's arm, provides direct access for administering medication. Adenosine is injected rapidly over a few seconds (rapid IV push), followed immediately by a saline flush to ensure quick and effective delivery into the bloodstream. The dosing guidelines for treating supraventricular tachycardia (SVT) in adults are as follows: Initial dose: 6 mg rapid IV bolus; Second dose: If ineffective within 1–2 minutes, a second dose of 12 mg may be given (Table 3). This activation is one-shot rather than continuous, requiring further decisions by medical personnel based on patient response.

In our FPGA implementation, delays are controlled using counters within Verilog always blocks triggered by clock edges. Saline flush activation lasts for 10 clock cycles following drug delivery (drug_delivery_activate), ensuring timely administration of medication. Similarly, IV-line setup is automatically deactivated after 20 clock cycles to complete the drug delivery process.

The FPGA simulation was conducted using Xilinx Vivado, with Verilog code programmed to model real-time decision-making based on patient heart rate and SpO_2 data. Heart rate values were simulated within a range of 30–150 bpm to cover bradycardia, tachycardia, and normal conditions. When bradycardia was detected (<50 bpm with SpO_2 <95%), the cpr_activate signal was asserted, triggering CPR actuation. Similarly, tachycardia detection (>120 bpm with SpO_2 ≥95%) asserted the drug_delivery_activate signal, initiating drug administration with dosage computed based on patient-specific parameters.

The simulation results of our test bench are shown in Fig. 5, where all values are presented in hexadecimal format. Figure 5 illustrates the output signals generated by the FPGA controller during simulation. These signals include cpr_activate, drug_delivery_activate, and drug_dosage, which dynamically adjust based on patient-specific parameters. Table 4 provides a breakdown of simulation results across different input conditions.

The FPGA simulation results demonstrate that CPR activation occurs only when bradycardia (<50 bpm) is detected alongside low oxygen saturation (<95%) and valid ECG signals. Similarly, drug delivery activation occurs within 10 ns of detecting tachycardia (>120 bpm), provided normal oxygen levels (≥95%) and valid ECG signals are present. These results validate the system's ability to avoid false positives by considering multiple physiological parameters. Simulations conducted in MATLAB confirm that LiDAR-based chest mapping achieves an average error margin of ±2 mm, ensuring precise alignment of CPR devices with patient contours. The observed behavior aligns with design logic, demonstrating reliability in detecting and responding to critical heart rate conditions.

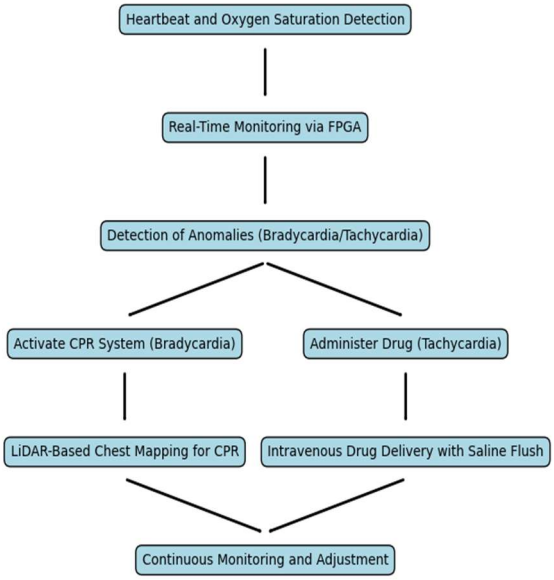

Figure 1: Flowchart of the proposed automatic CPR system with inbuilt drug delivery

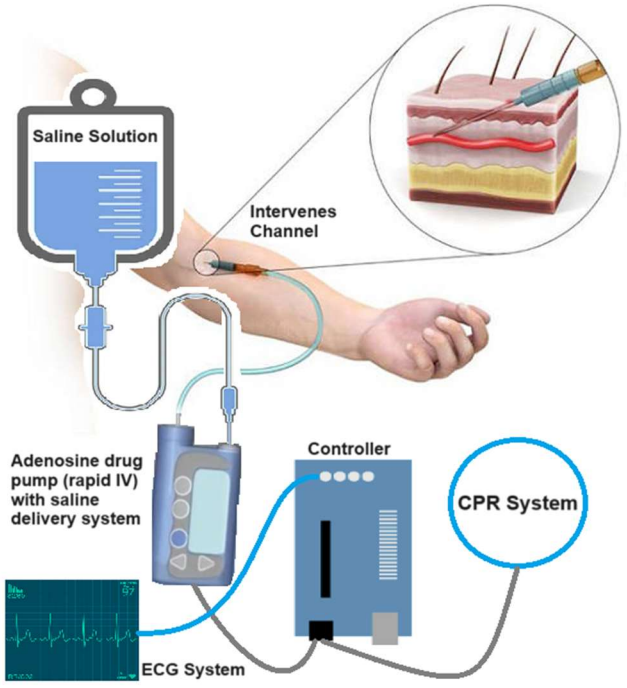

Figure 2: Block diagram of the proposed automatic CPR system with intravenous drug delivery system

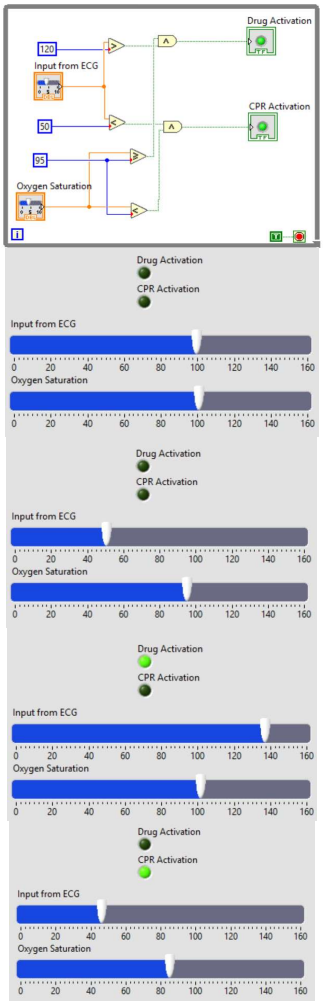

Figure 3: Workflow of the FPGA controller for real-time decision-making based on heart rate and oxygen saturation (SpO_2) levels. The system uses two comparators to detect bradycardia (<50 bpm with SpO_2 <95%) and tachycardia (>120 bpm with SpO_2 ≥95%), triggering either CPR activation or drug delivery respectively. When heart rate and SpO_2 are within normal ranges, the controller remains inactive. The diagram illustrates how the FPGA processes ECG data and controls interventions, including CPR actuation and intravenous drug administration, based on patient-specific conditions.

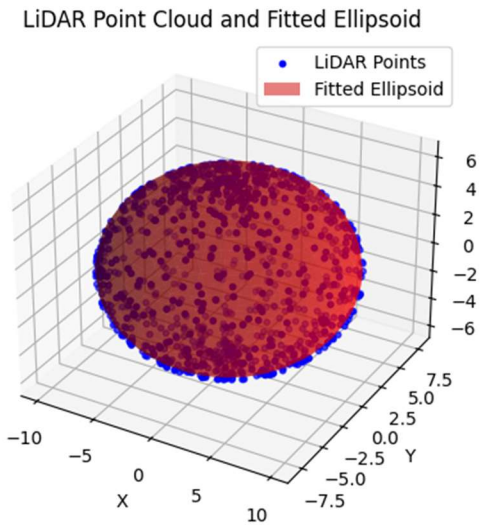

Figure 4: 3D ellipsoid model generated by LiDAR to target the CPR area of the patient using MATLAB

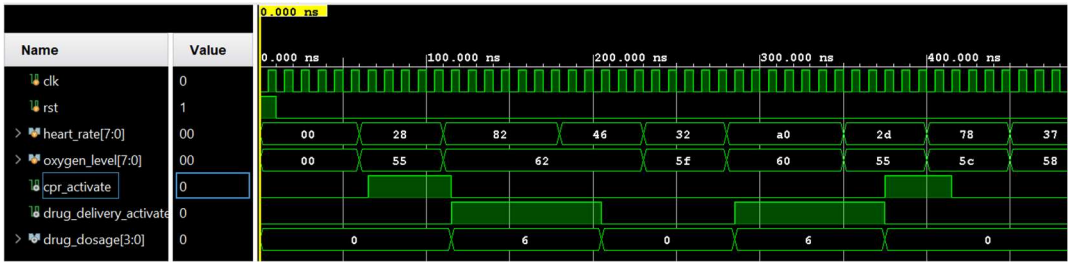

Figure 5: FPGA simulation results showing activation signals (cpr_activate and drug_delivery_activate) based on multi-parameter decision-making using heart rate thresholds, oxygen saturation levels (SpO_2), and ECG signal validity. The cpr_activate signal is triggered for bradycardia (<50 bpm with SpO_2 <95%), while the drug_delivery_activate signal is asserted for tachycardia (>120 bpm with SpO_2 ≥95%). The drug_dosage output dynamically adjusts based on simulated patient weight and age, ensuring personalized treatment. All values in the simulation results are presented in hexadecimal format.

Table 1: All system blocks interconnection

Unit	**Connected with**
ECG-Sensors	Data Processor
Data Processor	Central Control Unit
Central Control Unit	1.Mechanical CPR Device (Control Unit)
	2.Drug Delivery Unit (Control Algorithms)
Drug Reservoirs	Precision Pumps
Precision Pumps	Intravenous Line to Patient

Table 2: LiDAR point cloud and fitted ellipsoid parameters

Fitted Ellipsoid Parameters	**Values**
Number of Points (N)	10,000
Center Coordinates (x_0, y_0, z_0)	(0.00,−0.01,−0.02) m
Semi-Axis Lengths (a, b, c)	(10.00,8.00,6.00) m
Orientation (Eigenvectors Q)	$\begin{bmatrix}1 & 0 & 0\\0 & 1 & 0\\0 & 0 & 1\end{bmatrix}$
Eigenvalues (λ_1, λ_2, λ_3)	(100.00,64.00,36.00)
Ellipsoid Equation	$\frac{(x-0.02)^2}{0.03^2}+\frac{(y-0.15)^2}{0.02^2}+\frac{(z-0.10)^2}{0.01^2}=1$

Table 3: Suggested drug delivery steps with amount and delay

Drug name	**Amount**	**Time to delivery**	**Delay for 2nd dose**
Adenosine (1st dose)	6 mg	1-2 sec	1-2 minutes
Saline reflux	10-20 mL	rapid	1-2 minutes
Adenosine (2nd dose)	12 mg	1-2 sec	-

Table 4: FPGA simulation result breakdown

Time (ns)	Heart Rate (bpm)	Oxygen Level (%)	ECG Signal Valid	CPR Activate	Drug Delivery Activate	Drug Dosage (mg)	Remarks
50	70	98	Yes	0	0	0	Normal range, no action
100	40	85	Yes	1	0	0	Bradycardia, CPR activated
150	130	98	Yes	0	1	6	Tachycardia, drug delivery
200	50	95	No	0	0	0	Invalid ECG, no action
250	70	88	Yes	1	0	0	Critical oxygen desaturation
300	50	95	Yes	0	0	0	Edge case: lower limit, no action
350	120	95	Yes	0	0	0	Edge case: upper limit, no action
400	125	97	Yes	0	1	6	Tachycardia, drug delivery

4. CONCLUSION

In conclusion, the auto CPR integrated with drug delivery module introduced here presents a novel solution that combines advanced control technology, mechanical actuation, and automated drug delivery to provide efficient and timely emergency medical care. Utilizing a LiDAR system to accurately map and fit the auto CPR device to the patient's chest, the project ensures precise and effective chest compressions. The integration of ECG sensors and a central control unit enables real-time monitoring of heart rate, and the initiation of CPR and drug delivery based on the patient's condition. The system not only improves the accuracy and responsiveness of CPR administration but also enhances patient outcomes during critical moments. The automated drug delivery unit, capable of administering adenosine and saline flushes, adds another layer of sophistication by ensuring that medications are delivered promptly and accurately. While this study is limited to simulations, the results validate the feasibility of real-time decision-making for cardiac support using an FPGA controller. Future work will involve prototyping and experimental validation using CPR manikins equipped with pressure sensors and intravenous drug delivery setups to measure response times and accuracy. Overall, this approach, if properly implemented and taken to the finish line, stands to revolutionize emergency response protocols, offering reliable and life-saving technology that can be deployed in various settings to save lives and in a very cost-effective way.

5. FUTURE WORK

Developing an integrated system for automated CPR and drug delivery presents several challenges, including the need for reliable sensors, robust algorithms for decision-making, and ensuring the proper drug doses based on patient’s other medical conditions. However, advancements in sensor technology, machine learning, and biomedical engineering provide significant opportunities to overcome these

challenges. By leveraging these technologies, the proposed system aims to enhance intraoperative cardiac care, offering a seamless response to life-threatening events and reducing the reliance on manual interventions. This study lays the groundwork for developing a fully functional automated cardiac support system. The next steps include:

- Obtain valuable feedback about our model from medical practitioners.
- Building a physical prototype incorporating LiDAR sensors, FPGA controllers, and mechanical CPR devices.
- Testing the system on CPR manikins equipped with pressure sensors to measure compression depth and force distribution. These experiments will validate whether LiDAR-guided adjustments improve therapeutic outcomes compared to traditional methods.
- Collaborating with medical professionals to evaluate system performance in real-world scenarios.

DISCLOSURES

All authors have nothing to declare. No human or animal subjects were used in this research project.

REFERENCES

[1] A. R. Panchal, J. A. Bartos, J. G. Cabañas, M. W. Donnino, I. R. Drennan, K. G. Hirsch, P. J. Kudenchuk, M. C. Kurz, E. J. Lavonas, P. T. Morley, B. J. O'Neil, "Part 3: Adult Basic and Advanced Life Support: 2020 American Heart Association Guidelines for Cardiopulmonary Resuscitation and Emergency Cardiovascular Care," Circulation, vol. 142, no. 16_Suppl_2, pp. S366-S468, Oct. 2020.

[2] A. L. Hallstrom, T. D. Rea, M. R. Sayre, J. Christenson, A. R. Anton, V. N. Mosesso, L. Van Ottingham, M. Olsufka, S. Pennington, L. J. White, S. Yahn, "Manual Chest Compression vs Use of an Automated Chest Compression Device During Resuscitation Following Out-of-Hospital Cardiac Arrest: A Randomized Trial," JAMA, vol. 295, no. 22, pp. 2620-2628, Jun. 2006.

[3] D. Smekal, E. Lindgren, H. Sandler, J. Johansson, S. Rubertsson, "CPR-Related Injuries After Manual or Mechanical Chest Compressions with the LUCAS™ Device: A Multicentre Study of Victims After Unsuccessful Resuscitation," Resuscitation, vol. 85, no. 12, pp. 1708-1712, Dec. 2014.

[4] I. Savelieva and J. Camm, "Anti-arrhythmic Drug Therapy for Atrial Fibrillation: Current Anti-arrhythmic Drugs, Investigational Agents, and Innovative Approaches," Europace, vol. 10, no. 6, pp. 647-665, Jun. 2008.

[5] G. P. Forlenza, B. Buckingham, D. M. Maahs, "Progress in Diabetes Technology: Developments in Insulin Pumps, Continuous Glucose Monitors, and Progress Towards the Artificial Pancreas," The Journal of Pediatrics, vol. 169, pp. 13-20, Feb. 2016.

[6] M. W. Wukitsch, M. T. Petterson, D. R. Tobler, J. A. Pologe, "Pulse Oximetry: Analysis of Theory, Technology, and Practice," Journal of Clinical Monitoring, vol. 4, pp. 290-301, Oct. 1988.

[7] J. R. Spiro, S. White, N. Quinn, C. J. Gubran, P. F. Ludman, J. N. Townend, S. N. Doshi, "Automated Cardiopulmonary Resuscitation Using a Load-Distributing Band External Cardiac Support Device for In-Hospital Cardiac Arrest: A Single Centre Experience of AutoPulse-CPR," International Journal of Cardiology, vol. 180, pp. 7-14, Feb. 2015.

[8] J. N. Siebert, F. Ehrler, C. Combescure, L. Lacroix, K. Haddad, O. Sanchez, A. Gervaix, C. Lovis, S. Manzano, "A Mobile Device App to Reduce Time to Drug Delivery and Medication Errors During Simulated Pediatric Cardiopulmonary Resuscitation: A Randomized Controlled Trial," Journal of Medical Internet Research, vol. 19, no. 2, p. e31, Feb. 2017.

[9] J. R. Spiro, S. White, N. Quinn, C. J. Gubran, P. F. Ludman, J. N. Townend, S. N. Doshi, "Automated Cardiopulmonary Resuscitation Using a Load-Distributing Band External Cardiac Support Device for In-Hospital Cardiac Arrest: A Single Centre Experience of AutoPulse-CPR," International Journal of Cardiology, vol. 180, pp. 7-14, Feb. 2015.

[10] J. N. Siebert, F. Ehrler, C. Combescure, L. Lacroix, K. Haddad, O. Sanchez, A. Gervaix, C. Lovis, S. Manzano, "A Mobile Device App to Reduce Time to Drug Delivery and Medication Errors During Simulated Pediatric Cardiopulmonary Resuscitation: A Randomized Controlled Trial," Journal of Medical Internet Research, vol. 19, no. 2, p. e31, Feb. 2017.

[11] J. P. Nolan, J. Soar, V. Wenzel, P. Paal, "Cardiopulmonary Resuscitation and Management of Cardiac Arrest," Nature Reviews Cardiology, vol. 9, no. 9, pp. 499-511, Sep. 2012.

[12] J. Yeung and G. D. Perkins, "Timing of Drug Administration During CPR and the Role of Simulation," Resuscitation, vol. 81, no. 3, pp. 265-266, Mar. 2010.

[13] A. Islam and D. M. Farid, "FPGA-based ECG signal processing for QRS detection and arrhythmia classification," IEEE Transactions on Biomedical Engineering, vol. 67, no. 8, pp. 2112-2123, 2020.
[14] S. Sharma, P. K. Verma, and S. Bhatia, "Real-time seizure detection using FPGA-implemented EEG signal analysis," Medical Engineering & Physics, vol. 83, pp. 10-20, 2021.
[15] J. Chen et al., "Wearable health monitoring system based on FPGA and Bluetooth technology," Sensors, vol. 20, no. 15, p. 4387, 2020.
[16] M. K. Nandhini et al., "FPGA-based image processing system for high-resolution ultrasound imaging," Biomedical Signal Processing and Control, vol. 67, p. 102556, 2021.
[17] Y. Wu et al., "A multi-parameter health monitoring system using FPGA and IoT integration," Journal of Medical Systems, vol. 44, no. 3, p. 52, 2020.
[18] I. Lee, B. Kim, S. W. Lee, K. Y. Lee, and H. Yi, "An FPGA-based embedded system for portable and cost-efficient biosensing: A low-cost controller for biomedical diagnosis," in 2015 IEEE International Circuits and Systems Symposium (ICSyS), 2015, pp. 1-6.
[19] D. S. Short, "The Syndrome of Alternating Bradycardia and Tachycardia," British Heart Journal, vol. 16, no. 2, pp. 208, Apr. 1954.
[20] S. Steen, Q. Liao, L. Pierre, A. Paskevicius, and T. Sjöberg, "Evaluation of LUCAS, a new device for automatic mechanical compression and active decompression resuscitation," *Resuscitation*, vol. 55, no. 3, pp. 285–299, 2002.
[21] X. Wang, H. Pan, K. Guo, X. Yang, and S. Luo, "The evolution of LiDAR and its application in high precision measurement," in IOP Conference Series: Earth and Environmental Science, vol. 502, no. 1, p. 012008, May 2020.
[22] A. J. Camm and C. J. Garratt, "Adenosine and Supraventricular Tachycardia," New England Journal of Medicine, vol. 325, no. 23, pp. 1621-1629, Dec. 1991.
[23] R. A. Ali, A. A. Gandhi, H. Meng, S. Yalavarthi, A. P. Vreede, S. K. Estes, O. R. Palmer, P. L. Bockenstedt, D. J. Pinsky, J. M. Greve, J. A. Diaz, "Adenosine Receptor Agonism Protects Against NETosis and Thrombosis in Antiphospholipid Syndrome," Nature Communications, vol. 10, p. 1916, Apr. 2019.
[24] K. Honarmand, C. Mepham, C. Ainsworth, Z. Khalid, "Adherence to Advanced Cardiovascular Life Support (ACLS) Guidelines During In-Hospital Cardiac Arrest is Associated with Improved Outcomes," Resuscitation, vol. 129, pp. 76-81, Aug. 2018.
[25] M. Saeed, Q. Wang, O. Märtens, B. Larras, A. Frappé, B. Cardiff, D. John, "Evaluation of Level-Crossing ADCs for Event-Driven ECG Classification," IEEE Transactions on Biomedical Circuits and Systems, vol. 15, no. 6, pp. 1129-1139, Dec. 2021.
[26] A. Cheng, L. L. Brown, J. P. Duff, J. Davidson, F. Overly, N. M. Tofil, D. T. Peterson, M. L. White, F. Bhanji, I. Bank, R. Gottesman, "Improving Cardiopulmonary Resuscitation with a CPR Feedback Device and Refresher Simulations (CPR CARES Study): A Randomized Clinical Trial," JAMA Pediatrics, vol. 169, no. 2, pp. 137-144, Feb. 2015.
[27] B. E. Marks, K. M. Williams, J. S. Sherwood, M. S. Putman, "Practical Aspects of Diabetes Technology Use: Continuous Glucose Monitors, Insulin Pumps, and Automated Insulin Delivery Systems," Journal of Clinical & Translational Endocrinology, vol. 27, p. 100282, Mar. 2022.
[28] S. E. Reutebuch, H. E. Andersen, R. J. McGaughey, "Light Detection and Ranging (LIDAR): An Emerging Tool for Multiple Resource Inventory," Journal of Forestry, vol. 103, no. 6, pp. 286-292, Sep. 2005.
[29] Y. Lyu, X. Huang, Z. Zhang, "EllipsoidNet: Ellipsoid Representation for Point Cloud Classification and Segmentation," in Proceedings of the IEEE/CVF Winter Conference on Applications of Computer Vision, 2022, pp. 854-864.
[30] M. Zijlmans, D. Flanagan, J. Gotman, "Heart Rate Changes and ECG Abnormalities During Epileptic Seizures: Prevalence and Definition of an Objective Clinical Sign," Epilepsia, vol. 43, no. 8, pp. 847-854, Aug. 2002.
[31] K. G. Reddy, P. A. Vijaya, S. Suhasini, "ECG Signal Characterization and Correlation to Heart Abnormalities," International Research Journal of Engineering and Technology (IRJET), vol. 4, no. 5, May 2017.
[32] N. L. McIntosh-Yellin, B. J. Drew, M. M. Scheinman, "Safety and Efficacy of Central Intravenous Bolus Administration of Adenosine for Termination of Supraventricular Tachycardia," Journal of the American College of Cardiology, vol. 22, no. 3, pp. 741-745, Sep. 1993.
[33] S. H. Lim, V. Anantharaman, W. S. Teo, Y. H. Chan, "Slow Infusion of Calcium Channel Blockers Compared with Intravenous Adenosine in the Emergency Treatment of Supraventricular Tachycardia," Resuscitation, vol. 80, no. 5, pp. 523-528, May 2009.